

Thermal Transitions in Dry and Hydrated Layer-by-Layer Assemblies Exhibiting Linear and Exponential Growth

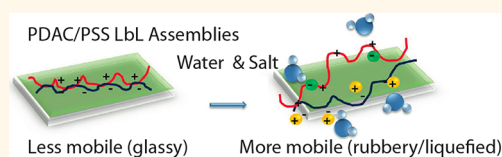
Ajay Vidyasagar,[†] Choonghyun Sung,[†] Randall Gamble,[‡] and Jodie L. Lutkenhaus^{†,*}

[†]Artie McFerrin Department of Chemical Engineering, Texas A&M University, College Station, Texas 77843, United States and [‡]Department of Chemical Engineering, University of Pittsburgh, Pittsburgh, Pennsylvania 15261, United States

Layer-by-layer (LbL) assemblies, which are nanoscale films made from the alternate adsorption of oppositely charged species, have found widespread applications in optics,¹ drug delivery,^{2,3} bioactive membranes,⁴ sensors,⁵ and conductive coatings.⁶ The growth and properties of LbL films are influenced by a number of parameters including ionic strength,^{7,8} salt-type,^{9–11} pH,^{12,13} solvent quality,¹⁴ temperature,^{15–17} and humidity.¹⁸ However, very little is known about the thermal behavior of LbL films, and knowledge of such properties is critical for understanding mechanical properties and the mechanism of LbL growth. For example, Lavalle *et al.*¹⁹ proposed that exponential growth was attributed to the diffusion of chains “in and out” of the film, and that linear growth was attributed to the inability of chains to diffuse within the time scale of adsorption. If such a hypothesis is true, then one might expect exponentially growing films to be more mobile or viscoelastic than linearly growing films; reflecting these differences in mobility, linearly growing films may possess a glass transition temperature (T_g) higher than that of exponentially growing films. Therefore, it is pertinent to understand thermal properties such as T_g , physical aging, and thermal cross-linking, but these are often difficult to measure because LbL films can be very thin.

Because LbL assemblies are grown in an aqueous environment, the thermal and mechanical properties of the hydrated film are of particular interest. Depending on assembly condition, LbL films can behave as either viscoelastic or rigid films.^{20–23} Several groups investigating the mechanical properties of LbL films have reported dramatic changes in modulus for dry *versus* hydrated

ABSTRACT



Layer-by-layer (LbL) assemblies are remarkable materials, known for their tunable mechanical, optical, and surface properties in nanoscale films. However, questions related to their thermal properties still remain unclear. Here, the thermal properties of a model LbL assembly of strong polyelectrolytes, poly(diallyldimethylammonium chloride)/poly(styrene sulfonate) (PDAC/PSS), assembled from solutions of varying ionic strength (0–1.25 M NaCl) are investigated using quartz crystal microbalance with dissipation (QCM-D) and modulated differential scanning calorimetry. Hydrated exponentially growing films (assembled from 0.25 to 1.25 M NaCl) exhibited distinct thermal transitions akin to a glass transition at 49–56 °C; linearly growing films (assembled without added salt) did not exhibit a transition in the temperature range investigated and were glassy. Results support the idea that exponentially growing films have greater segmental mobility than that of linearly growing films. On the other hand, all dry LbL assemblies investigated were glassy at room temperature and did not exhibit a T_g up to 250 °C, independent of ionic strength. For the first time, thermal transitions such as T_g values can be measured for LbL assemblies using QCM-D by monitoring fluctuations in changes in dissipation, allowing us to probe the film's internal structure as a function of film depth.

KEYWORDS: glass transition · polyelectrolyte multilayers · layer-by-layer assembly · modulated differential scanning calorimetry · quartz crystal microbalance with dissipation

films;^{18,24–32} these findings suggest that water, acting as a plasticizer, lowers the glass transition temperature (T_g) and increases viscoelasticity.

Several noteworthy contributions to the thermal analysis of LbL assemblies have focused on a system of strong polyelectrolytes, positively charged poly(diallyldimethylammonium chloride) (PDAC), and negatively charged polystyrene sulfonate (PSS).

* Address correspondence to jodie.lutkenhaus@che.tamu.edu.

Received for review April 6, 2012 and accepted June 6, 2012.

Published online June 06, 2012
10.1021/nn301526b

© 2012 American Chemical Society

Mueller *et al.*³³ reported a decrease in modulus of 2 orders magnitude at 35 °C for hydrated PDAC/PSS LbL capsules terminated with PSS. Köhler *et al.*³⁴ reported that hydrated PDAC/PSS LbL capsules terminated with PSS shrank at 35–40 °C upon heating, which was attributed to a glassy-to-viscoelastic melting process observed using microdifferential scanning calorimetry. Nazaran *et al.*³⁵ observed an increase in lateral mobility of 1–2 orders of magnitude for PDAC/PSS LbL assemblies terminated with PDAC at 65 °C, which was attributed to a thermal transition. Historically, this transition has been termed a “glass transition” and has been thought to arise from the breaking of ion pairs and subsequent chain relaxation. Ghostine and Schlenoff³⁶ reported that for hydrated PDAC/PSS LbL films terminated with PSS in the presence of ferricyanide probing ions, the diffusion coefficient of ferricyanide within the film increased with increasing temperature (15 to 50 °C); however, no clear phase transition was observed. Considering that mobility and T_g are related, it is reasonable that temperature should influence whether LbL assemblies grow linearly or exponentially. Salomäki *et al.*³⁷ observed that PDAC/PSS LbL films assembled from 0.1 M NaBr transitioned from linear growth at 15 and 25 °C to exponential growth at 45 and 55 °C.

The prior results collectively suggest that relaxation of and diffusion within hydrated PDAC/PSS LbL assemblies are highly sensitive to temperature. On the other hand, the prior work also points to the inherent difficulty in reliably measuring transition temperatures in LbL assemblies, motivating us to investigate thermal transitions in dry and hydrated PDAC/PSS LbL assemblies exhibiting linear and exponential growth. Recently, we demonstrated that dry poly(allylamine hydrochloride)/poly(acrylic acid) PAH/PAA LbL films were glassy at room temperature, and that they cross-linked at elevated temperatures before any measurable T_g could be detected.^{38,39} In earlier work, dry hydrogen bonding polyethylene oxide/PAA LbL films had a T_g between that of its homopolymer constituents.^{40–42} Despite these recent advances, key questions remain regarding the influence of hydration and ionic strength on thermal properties and regarding their relationship with the mechanism of linear and exponential film growth.

In this present work, we investigate two complementary methods of detecting glass transition temperatures in LbL films. PDAC/PSS LbL assemblies are chosen as the model system because they grow linearly or exponentially, depending on ionic strength, and because they are popularly studied strong polyelectrolytes. Hydrated PDAC/PSS LbL thin films (70–300 nm) are examined using temperature-controlled quartz crystal microbalance with dissipation (QCM-D), and free-standing dry and hydrated bulk PDAC/PSS LbL assemblies (1–1.5 μm) are examined

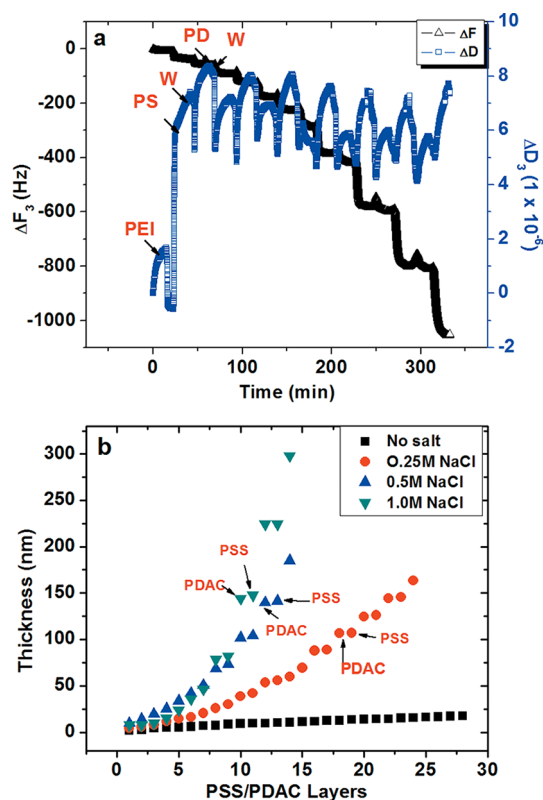


Figure 1. (a) Frequency and dissipation changes for PEI/(PSS/PDAC)₇ LbL films assembled from 0.5 M NaCl during LbL film deposition (PD/PDAC, PS/PSS, W/rinse). (b) Hydrated thickness as a function of layer number for PEI-(PDAC/PSS) LbL films assembled from 0, 0.25, 0.5, and 1.0 M NaCl. The initial PEI layer is taken as the zeroth layer.

using modulated differential scanning calorimetry (MDSC). The former technique is particularly novel in that it has never before been used to detect thermal transitions in LbL assemblies. QCM-D provides us with a novel route to accurately probe such transitions for ultrathin polymer films *via* changes in both hydrated film mass and viscoelasticity as a function of film depth. The technique is not limited to LbL assemblies but can potentially be used to detect thermal transitions universally in different polymeric systems. Results indicate that hydrated exponentially growing PDAC/PSS LbL films have T_g values around 49–56 °C, whereas linearly growing assemblies do not have a detectable glass transition and are glassy at room temperature. Both linearly and exponentially growing LbL assemblies in the dry state do not have a detectable T_g and are glassy at room temperature. Results support the hypothesis that exponentially growing films have more mobility relative to linearly growing films, allowing for greater interdiffusion of polyelectrolytes among layers during the assembly process.

RESULTS

We performed QCM-D experiments on select PDAC/PSS LbL assemblies assembled from solutions of 0 to 1.25 M NaCl, where polyethyleneimine (PEI) was added

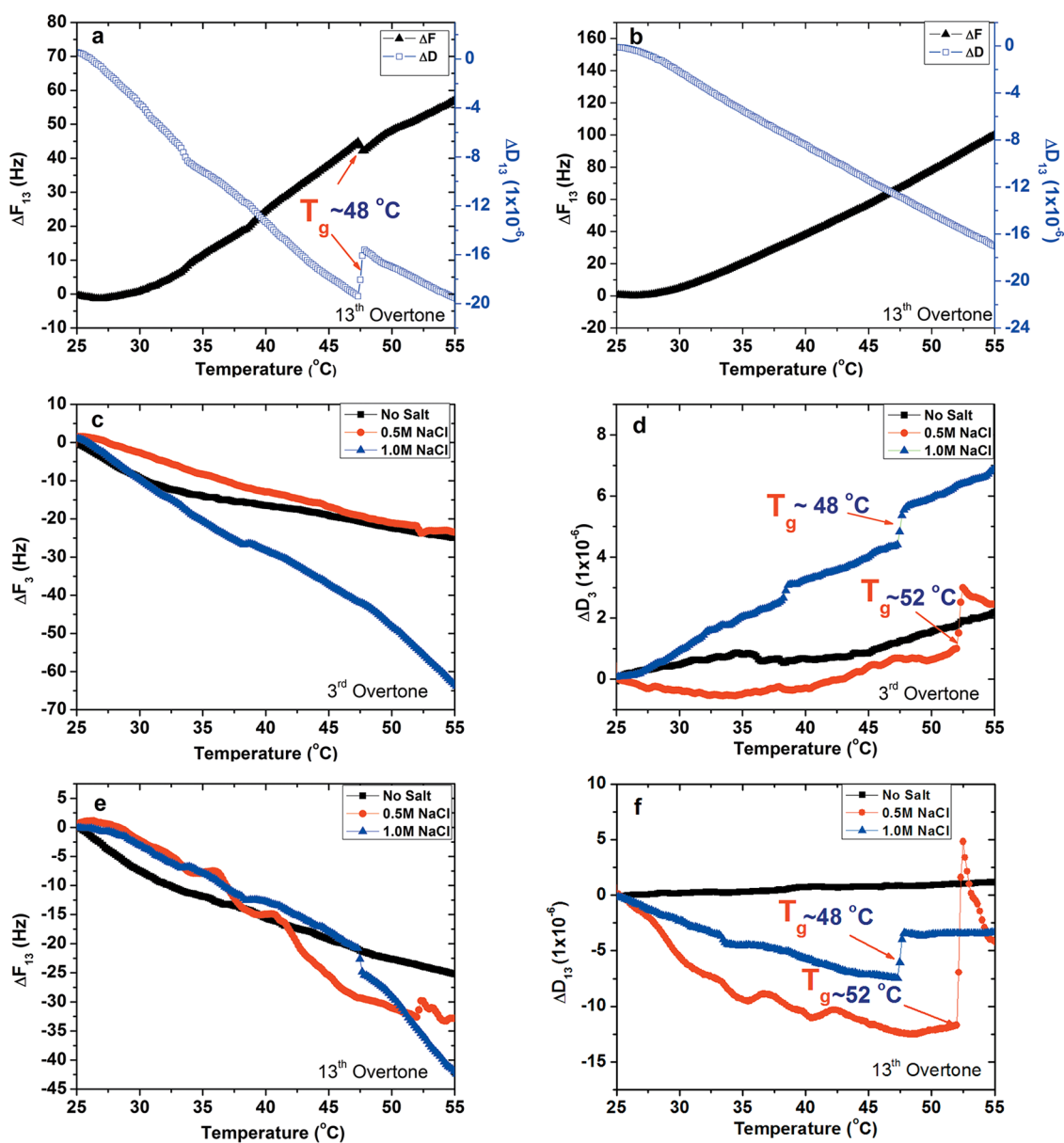


Figure 2. Temperature dependence of ΔF and ΔD for the 13th overtone of (a) PEI/(PSS/PDAC)₇ LbL films assembled from 1.0 M NaCl (uncorrected) and (b) for the bare crystal immersed in 1.0 M NaCl. Temperature dependence of corrected ΔF (c,e) and ΔD (d,f) for PEI/(PSS/PDAC)₇ LbL films assembled from 0, 0.5, and 1.0 M NaCl. The third overtones are shown in (c,d), and the 13th overtones are shown in (e,f). Heating at a rate of 1 $^{\circ}\text{C}/\text{min}$.

as an initial layer to promote adsorption. Our motivation was to examine if ionic strength (or linear vs exponential growth) affects T_g . As solutions of PDAC and PSS were alternately flowed over a quartz crystal, changes in frequency (ΔF) and dissipation (ΔD) were monitored. Figure 1a shows the response for a typical build up of a PEI/(PSS/PDAC)₇ LbL film assembled from 0.5 M NaCl, where the subscript denotes the number of layer pairs deposited. A decrease in ΔF indicates that the mass of the hydrated film adsorbed on the crystal increases, and an increase in ΔD indicates that the viscoelasticity of the film increases. As the number of layers increased, ΔF decreased, confirming LbL film growth. ΔD increased after the first bilayer and then

oscillated over a constant value. The relatively low ΔD value indicates that the film is somewhat rigid, as suggested by others.^{43,44} Using the Sauerbrey mass and thickness as an initial guess, we calculated mass and thickness changes using a Voigt viscoelastic model (Figure 1b and Table S1). Exponential growth was observed for 0.25, 0.5, and 1.0 M NaCl assembly solutions, and linear growth was observed for the case of no added salt, which matches previous reports.^{7,8} For the 0.25, 0.5, and 1.0 M NaCl assembly conditions, PDAC mass increased far more relative to PSS mass during their respective adsorption steps. Such behavior has been reported elsewhere and is associated with exponential growth.^{8,43–45}

Following assembly, temperature-controlled QCM-D was used to observe changes in frequency and dissipation for PEI(PSS/PDAC) LbL films assembled from 0, 0.25, 0.5, and 1.0 M NaCl solutions with PDAC as the terminal layer. During the experiment, LbL films were submerged in water of ionic strength matching their assembly conditions, and samples were ramped from 25 to 55 °C at 1 °C/min except in the case of LbL films assembled from 0.25 M NaCl, wherein the temperature was ramped from 25 to 65 °C. Figure 2a shows raw frequency and dissipation changes for the 13th overtone for PEI(PSS/PDAC)₇ LbL films assembled from 1.0 M NaCl, which includes the response of not only for the LbL film but also for the bare crystal. The temperature-dependent response of the bare crystal submerged in 1.0 M NaCl is shown in Figure 2b. Because the density and viscosity of water are also functions of temperature, so is the submerged crystal's response.⁴⁶ To isolate the response of the LbL film alone, the changes in frequency and dissipation of the bare crystal were subtracted from the raw frequency and dissipation changes of the LbL assemblies, resulting in Figure 2c–f.

One unique feature of QCM-D is the ability to probe changes in frequency and dissipation at various penetration depths using overtones. Various overtones have penetration depths dependent on the decay length of the evanescent wave in contact with the film and the contacting fluid. Lower overtones have a larger penetration depth compared to higher overtones. For instance, for water at 20 °C, the penetration depth of the evanescent wave is ~145 nm from the crystal–film interface for the third overtone compared to ~50 nm for the 13th overtone. In other words, lower overtones probe deeper into the film, whereas higher overtones are more sensitive to the film closer to the crystal–film interface.^{47,48} Figure 2c,d shows changes in corrected frequency and dissipation for the third overtone for PEI(PSS/PDAC) LbL films terminated with PDAC and assembled from 0, 0.5, and 1.0 M NaCl. For all ionic strengths explored, the corrected ΔF decreased with increasing temperature, suggesting an increase in hydration. For LbL films assembled from 0.5 and 1.0 M NaCl, a distinct step change in ΔD was observed at 52 and 48 °C, respectively, where ΔD abruptly increased by 1 to 2×10^{-6} units, indicating a sudden increase in viscoelasticity. The magnitude of the step change associated with the transition was greater than the noise, allowing us to accurately measure the transition itself. In contrast, no step-change in ΔD was observed for LbL films assembled without added salt. Generally for each of the four cases explored, ΔD slightly increased with temperature.

Figure 2e,f shows changes in corrected frequency and dissipation for the 13th overtone for PEI(PSS/PDAC) LbL films terminated with PDAC assembled from 0, 0.5, and 1.0 M NaCl. Similar to data from the third overtone, ΔF decreased with increasing temperature,

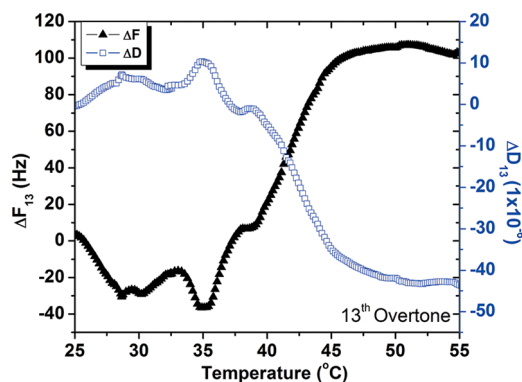


Figure 3. Temperature dependence for corrected ΔF and ΔD for a PEI(PSS/PDAC)_{7.5} LbL film assembled from 0.5 M NaCl (13th overtone).

and step changes in ΔD were observed for films assembled from 0.5 and 1.0 M NaCl at temperatures coinciding with the transitions previously observed. The magnitude of the step change for the 13th overtone was much larger, where ΔD increased by 15×10^{-6} and 4×10^{-6} units, compared to the third overtone for films assembled from 0.5 and 1.0 M NaCl, respectively. In other words, the transition was more prominent closer to the crystal–film interface. Unlike the third overtone's response, dissipation decreased up to the step change with increasing temperature, indicating that the film near the crystal–film interface became more rigid prior to the transition. The *absolute* values of ΔD for PDAC/PSS LbL films assembled from 0.5 and 1.0 M NaCl varied from sample to sample. However, the overall *trend* in ΔD remained consistent, and the temperature of the step change was reproducible from sample to sample. No step change in ΔD was observed for films assembled without added salt.

The step change in ΔD observed for exponentially growing LbL films using QCM-D is likely attributed to a thermal transition associated with the breaking of ion pairs and subsequent chain relaxation, resulting in a more viscoelastic film. The temperature for the glassy–viscoelastic transition observed in QCM-D coincides with the T_g observed using MDSC. For linearly growing films, no thermal transition was observed in both QCM-D and MDSC. Results from films assembled from 1.25 M NaCl were unreliable because of noise in both ΔF and ΔD owing to film delamination. Some exponentially growing LbL films undergo microphase separation owing to the temperature-activated diffusion of polymer chains.⁴⁹ However, in this present study, optical microscopy of PEI(PSS/PDAC) LbL films indicated no phase separation or dewetting upon heating (Figure S1).

Unique behavior was observed for films assembled from 0.25 M, where characteristics of both linearly and exponentially growing films were observed (Figure S2b). Growth was exponential but far less so than films assembled at higher ionic strengths (Figure 1).

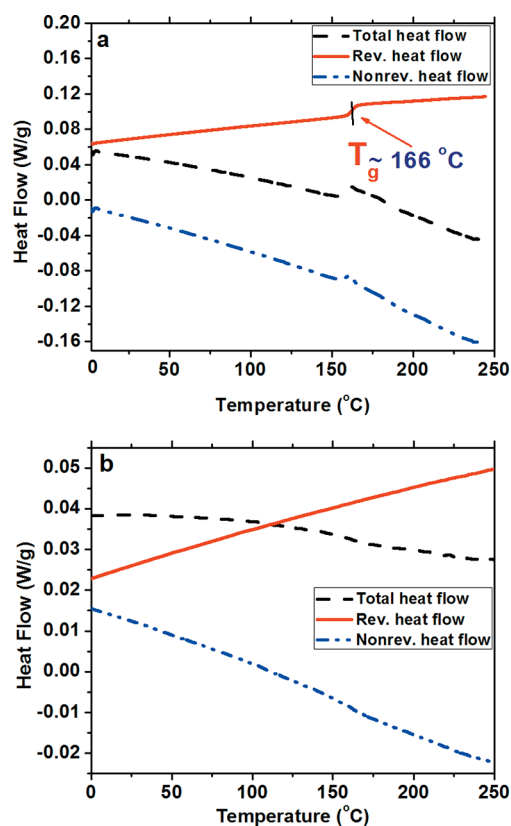


Figure 4. MDSC thermograms of (a) dry PDAC and (b) dry PSS homopolymers (second heating scan). Ramped at $3\text{ }^{\circ}\text{C min}^{-1}$, amplitude of $1\text{ }^{\circ}\text{C}$, period of 60 s.

From the third overtone, the step changes in ΔF and ΔD for PEI/(PSS/PDAC) LbL films assembled from 0.25 M NaCl terminated with PDAC were only detected from repeated cooling cycles ($56\text{ }^{\circ}\text{C}$) and were small in magnitude, indicating that the transition is rather weak. In the 13th overtone, the transitions were nearly nonexistent. These observations suggest that this assembly condition represents a tipping point for linear to exponential growth and behavior.

Because several reports^{33,34,50,51} indicate that the terminal layer can have a dramatic effect on the temperature response in PDAC/PSS LbL capsules, we desired to explore this so-called “odd–even” phenomenon by performing QCM-D with PSS as the terminal layer. Figure 3 shows the temperature response for a PEI/(PSS/PDAC)_{7.5} LbL film (initially 191 nm thick) assembled from 0.5 M NaCl, where the general trends are distinctly different from Figure 2, where PDAC was the terminal layer. ΔF and ΔD for LbL films terminated with PSS fluctuated around a constant value from 25 to 35 $^{\circ}\text{C}$. Upon further heating from 35 to 45 $^{\circ}\text{C}$, ΔF abruptly increased and ΔD abruptly decreased. During this transition, the hydrated mass decreased and the film became more rigid. At higher temperatures (45–55 $^{\circ}\text{C}$), both ΔF and ΔD remained more or less constant. The transitions observed here for thin PDAC/PSS films complement prior reports,^{33,50,52} where PDAC/PSS LbL

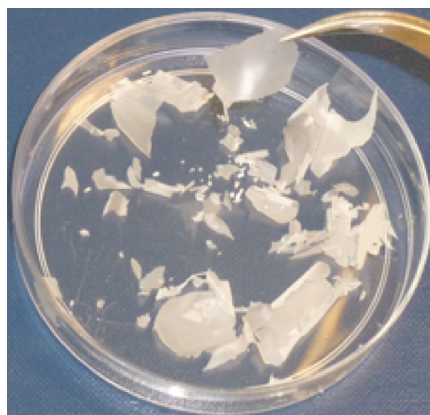


Figure 5. Free-standing dry PDAC/PSS LbL film assembled from 1.0 M NaCl.

capsules swell with increasing temperature if PDAC is the terminal layer, but capsules shrink if PSS is the terminal layer.

To corroborate QCM-D findings, MDSC experiments were performed on dry homopolymers PDAC and PSS and PDAC/PSS LbL films assembled with and without salt. MDSC is especially useful for sensitively and accurately measuring weak glass transitions. A modulated temperature ramp allows for separation of the reversing and nonreversing heat flows. Reversing heat flow captures phenomena (T_g , changes in C_p) at time scales shorter than the modulation period; nonreversing heat flow captures phenomena (aging, reactions) at time scales longer than the modulation period. We restrict our focus mainly to the reversible heat flow because most nonreversing heat flow curves were featureless, unless otherwise noted.

Figure 4 shows the second MDSC heating cycle for dry homopolymers PDAC and PSS. From the inflection point in the reversing curve, dry PDAC homopolymer exhibited a T_g at $170 \pm 4\text{ }^{\circ}\text{C}$; this T_g was accompanied by a small peak in the nonreversing curve, which we attribute to enthalpic relaxation associated with aging (Figure 4a). On the other hand, dry homopolymer PSS did not exhibit a T_g in the temperature range investigated (Figure 4b). Hydrated (12 wt % water) homopolymers PSS and PDAC were evaluated from 5 to 110 $^{\circ}\text{C}$ and did not have detectable T_g values, either (Figures S3 and S4). Therefore, the “hydrated” T_g of the homopolymers may lie above 110 $^{\circ}\text{C}$ or below 5 $^{\circ}\text{C}$, but we cannot directly confirm this using our present techniques. It is more likely that the T_g is above 110 $^{\circ}\text{C}$, given our own observations, where both polymers remained brittle even when slightly hydrated.

Next, we examined PDAC/PSS LbL films assembled onto Teflon from solutions of ionic strengths ranging from 0 to 1.25 M NaCl. PDAC/PSS LbL films were assembled until the film thickness was 1–1.5 μm . The isolated LbL films were brittle and flaky (Figure 5). Interestingly, even though dry homopolymer PDAC has a well-defined T_g , dry PDAC/PSS LbL films did not

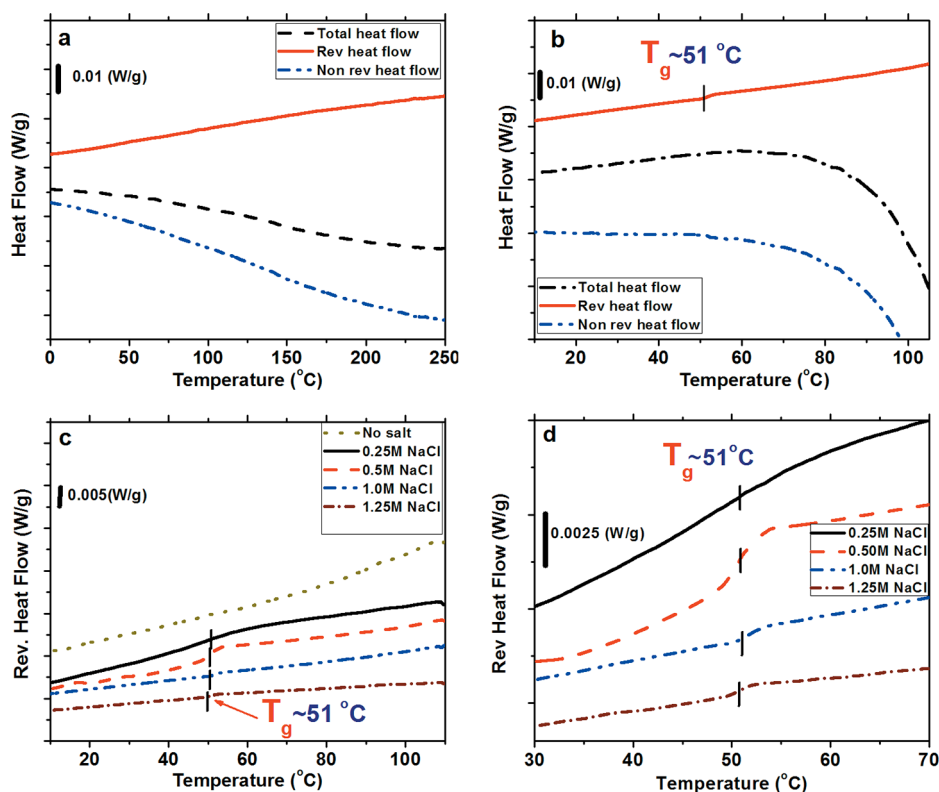


Figure 6. (a) MDSC thermogram of dry and (b) hydrated PDAC/PSS LbL films assembled from 1.0 M NaCl. (c) Reversing heat flow for hydrated PDAC/PSS LbL films assembled from 0 to 1.25 M NaCl, and (d) an expanded view of (c). Curves have been shifted along the y-axis for clarity. Cooling at $2\text{ }^{\circ}\text{C min}^{-1}$, amplitude of $1.272\text{ }^{\circ}\text{C}$ for 60 s.

TABLE 1. T_g Values for PDAC/PSS LbL Films and Homopolymers in Dry and Hydrated States

	dry (MDSC) T_g ($^{\circ}\text{C}$)	hydrated (12 wt % H_2O , MDSC) T_g ($^{\circ}\text{C}$)	hydrated (12 wt % H_2O , QCM-D) T_g ($^{\circ}\text{C}$)
PDAC homopolymer	170 ± 4	<i>a</i>	N/A
PSS homopolymer	<i>a</i>	<i>a</i>	N/A
PDAC/PSS (no salt)	<i>a</i>	<i>a</i>	<i>a</i>
PDAC/PSS (0.25 M NaCl)	<i>a</i>	52 ± 5	$56 \pm 2^{b,c}$
PDAC/PSS (0.5 M NaCl)	<i>a</i>	51.0 ± 0.2	53 ± 1^b
PDAC/PSS (1.0 M NaCl)	<i>a</i>	52 ± 1	49 ± 3^b
PDAC/PSS (1.25 M NaCl)	<i>a</i>	51.0 ± 0.6	delaminated

^a Not detectable in the temperature range investigated. ^b PDAC was the terminal layer. ^c Cooling cycle.

have a detectable T_{gr} , regardless of the ionic strength of the assembly solution (Figure 6a). The dry films likely have T_g values higher than the maximum temperature investigated, considering that the films were brittle at room temperature. We attribute the dry film's glassy behavior to strong ion pairing between quaternary ammonium and sulfonate groups.

In contrast to dry films, the behavior of PDAC/PSS LbL films hydrated in 12 wt % of their respective assembly solutions was quite different. Figure 6b shows an example of a MDSC thermogram for a hydrated PDAC/PSS LbL film assembled from 1.0 M NaCl. A clear thermal transition at $51\text{ }^{\circ}\text{C}$ was observed in the reversing curve. Figure 6c shows MDSC thermograms of hydrated PDAC/PSS LbL films assembled from 0 to 1.25 M NaCl. There was no significant deviation in

T_g with respect to ionic strength (0.25 to 1.25 M NaCl), except for films assembled without added salt, where no T_g was observed. Figure 6d shows an expanded view of the transitions, all of which are weak. No odd–even effect was observed for MDSC samples (Figure S5), in contrast to QCM-D experiments, suggesting that such an effect occurs for only thin samples. Table 1 summarizes findings from both MDSC and QCM-D experiments.

DISCUSSION

Temperature-controlled QCM-D and MDSC allow for the direct measurement of thermal transitions in LbL assemblies, which we have demonstrated using a model system of strong polyelectrolytes, PDAC/PSS. The following discussion will address the thermal

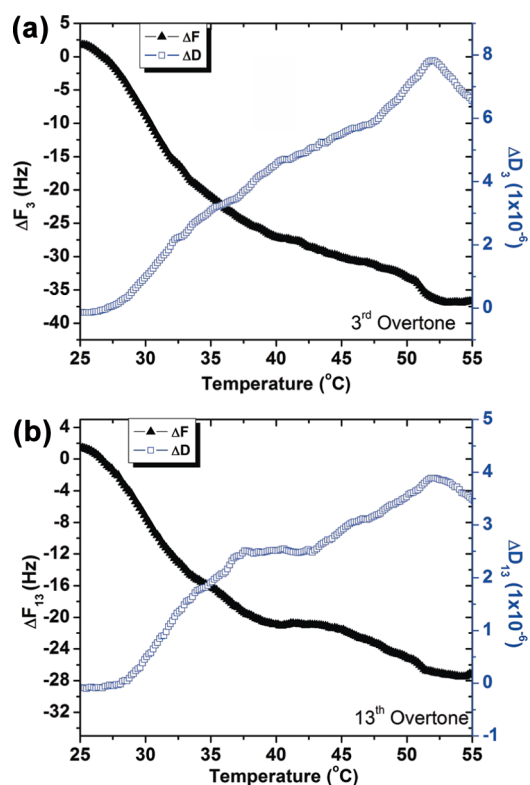


Figure 7. Corrected ΔF and ΔD as a function of temperature for PEI/(PSS/PDAC)₃ LbL films assembled from 1.0 M NaCl for the (a) third and (b) 13th overtones.

properties of thin LbL films measured using QCM-D and those of thick LbL films measured using MDSC as they relate to growth mechanism, confinement effects, and internal structure.

QCM-D in combination with MDSC provides detailed information on film hydration and viscoelasticity of PDAC/PSS LbL films during the glass transition. QCM-D is not commonly employed to probe glass transitions, but one report by Forrest *et al.* studied the relaxation dynamics for poly(styrene) thin films modified with silicon carbide nanoparticles using QCM-D by monitoring the changes in the dissipation as a function of film thickness.⁵³ Naturally, this technique is a potentially valuable tool for studying the effect of confinement on thin films and could be useful for polymers beyond just LbL assemblies.

One unique aspect of QCM-D is that the various overtones give insight into the LbL film's structure at various penetration depths relative to the crystal–film interface, so that different regions can be probed. The third overtone penetrates more deeply into the film and yields a response that is averaged over that particular depth, sampling both film close to the crystal–film interface and interior. On the other hand, the 13th overtone penetrates less deeply into the film, and the response is dominated more by film close to the crystal–film interface. The trend in ΔD with temperature is particularly different for the third and 13th overtones (Figure 2). With films assembled from 1.0 M

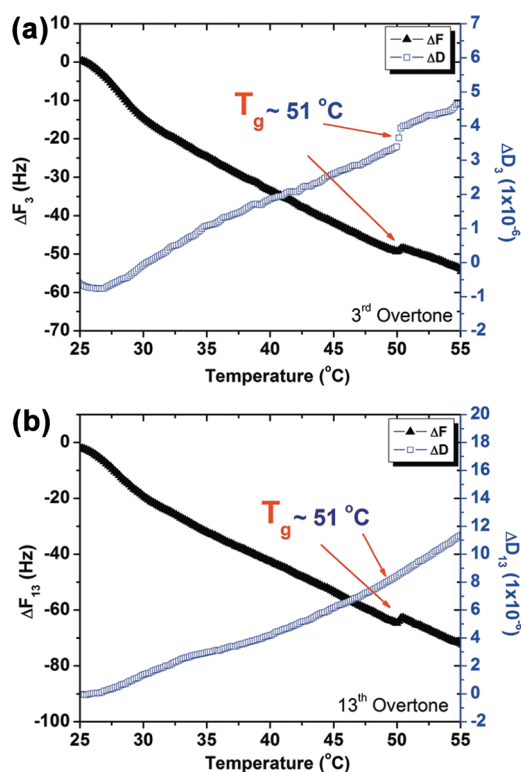


Figure 8. Corrected ΔF and ΔD as a function of temperature for PEI/(PSS/PDAC)₅ assembled in 1.0 M NaCl for the (a) third and (b) 13th overtone.

NaCl as an example, ΔD generally increases with temperature for the third overtone but decreases with temperature for the 13th overtone. These results suggest that film close to the crystal (13th overtone) becomes more rigid, whereas the interior film (3rd overtone) becomes more viscoelastic as temperature increases. In both overtones, the T_g was characterized by a sudden increase in ΔD , but the magnitude of the transition was larger for the 13th overtone relative to the third overtone. In other words, structural rearrangement close to the substrate was larger than that of the interior of the film. This finding may be explained by a recent neutron reflection study,⁵⁴ which measured a larger surface roughness in layers closer to the substrate than in the bulk. Those layers closer to the substrate were more interdigitated and intermixed than layers farther away from the substrate.

Considering that the growth of the first few layer pairs proceeds differently from subsequent layers, one might expect variance in structure and thermal behavior with respect to number of layer pairs. To test this hypothesis, QCM-D was performed on three and five layer pairs of hydrated PEI/(PSS/PDAC) LbL films terminated with PDAC and assembled from 1.0 M NaCl (Figures 7 and 8). For a film of three layer pairs (58 nm), no T_g was observed; however, for a film of five layer pairs (230 nm), a weak T_g at 51 °C was present. PDAC/PSS LbL films with few layer pairs may not exhibit a T_g either because of (i) polymer–substrate interactions,

which could limit segmental relaxations, or (ii) differences in the structure of the film between early and later stages of growth. The latter is possible considering that the number of water molecules per ion pair varies with the number of layer pairs; the first few layer pairs have less water, and water content stabilizes after the eight layer pair.⁵⁵ In our present work, we consistently observe T_g values in analogous films of seven layer pairs or more. This result suggests that water, which plasticizes the film, plays a significant role in the thermal transition.

Considering that an LbL film comprises two components, it is important to consider the thermal properties of the components themselves. MDSC thermograms (Figure 4a) show that PDAC homopolymer exhibits a well-defined glass transition at 170 ± 4 °C. This value is considerably higher than a previous report,⁵⁶ where a T_g of 68 °C was found for PDAC of an unspecified molecular weight; therefore, such a difference may possibly be explained by differences in molecular weight. For PSS, no T_g was observed in the temperature range investigated (0–250 °C) (Figure 4b). Several researchers have also reported similar results,^{57,58} where a T_g for PSS was not directly observed. In the absence of a direct measurement, M'Bareck *et al.* inferred the T_g of PSS from blend data using the Fox equation, estimating a value of 211 °C. Imre *et al.*⁵⁸ report a T_g of 180 °C for PSS measured directly using DSC. Surprisingly, dry PDAC/PSS LbL films did not exhibit a T_g for all ionic strengths investigated (Figure 3a). In contrast, dry PDAC/PSS polyelectrolyte complexes possessed T_g values between 90 and 143 °C, depending on stoichiometry.⁵⁸ This difference suggests that PDAC/PSS LbL films may have a structure dissimilar from analogous polyelectrolyte complexes. We chose to limit our temperature range to 250 °C because prior work by Farhat *et al.* reports that PDAC/PSS LbL assemblies degrade at 300 °C,⁵⁹ so the T_g for the dry LbL film may be above 250 °C.

The fact that MDSC and QCM-D show different trends in T_g with respect to ionic strength is indicative of the relative sensitivity of the instrumentation. For example, we found that QCM-D was far more sensitive to thermal transitions in LbL assemblies, yielding reproducible results upon multiple heating and cooling cycles across different samples and upon repeated cycling. On the other hand, transitions in LbL assemblies observed using MDSC were reproducible only upon cooling. Therefore, the trend in T_g with respect to ionic strength is most accurately measured using QCM-D, which showed that the transition temperature decreased from 56 to 49 °C as the assembly solutions' ionic strength increased from 0.25 to 1.0 M NaCl. As the ionic strength increases, the number of ion pairs within the film decreases because of shielding; segmental mobility increases, and T_g decreases. To examine if the ionic strength of the immersion solution influences the thermal properties, a PDAC/PSS LbL film assembled

from 1.0 M NaCl was immersed in water without added salt and MDSC was performed; a T_g at 51 °C was still present (Figure S5).

The T_g value for hydrated PDAC/PSS LbL films assembled from salt (49–56 °C) observed herein lies within the range of transition values observed using other techniques (35–65 °C) but is somewhat higher than analogous LbL capsules.^{24,33–36,60–62} This difference may be attributed to the odd–even effect often observed for capsules, where electrostatic and hydrophobic interactions compete to control whether the film swells or shrinks upon heating. In this present work, the odd–even effect was observed for thin films (170–300 nm) but not for thick films (1–1.3 μ m). Thin LbL films terminated with PSS shrank at 35 °C (Figure 3), similar to PSS-terminated capsules.^{34,51} On the other hand, an analogous thin LbL film terminated with PDAC swelled and became more hydrated upon heating (Figure 2). As suggested by Köhler *et al.*,^{34,50,51} PSS-terminated LbL capsules are dominated by hydrophobic interactions, and PDAC-terminated LbL capsules are dominated by electrostatic interactions. Increasing temperature enhances hydrophobic interactions but also encourages polyelectrolyte dissociation.⁶⁰ Possible reasons for differences in the thermal properties of capsules and films include the following: (i) capsules have a larger surface area exposed to water relative to flat films, allowing for rapid hydration; (ii) capsules have unrestricted movement facilitating greater thermal expansion or contraction, whereas flat LbL films are restricted by the substrate; and (iii) capsules, which are assembled from just a few layer pairs, may have a significant contribution from extrinsic charge compensation within the capsule shell.^{11,34,51,61}

The observed phenomenon is also related to the “glass transition ionic strength” concept.^{62–64} Kovacevic *et al.*⁶³ studied the formation and dissolution of LbL films containing weak polyelectrolytes as a function of ionic strength. At some critical ionic strength, c_g , the film transitioned from stepwise growth to growth with overshoots, which indicates initial formation of complexes at the surface and slow dissolution of those complexes. The critical ionic strength at which this growth transition occurred was termed the “glass transition ionic strength”. At ionic strengths less than c_g , the film was glass-like, while at ionic strengths higher than c_g , the film was liquid-like. Similarly, Chollakup *et al.*⁶⁰ demonstrated that polyelectrolyte complexes formed solid-like precipitates or liquid-like coacervates at lower ionic strengths or higher ionic strengths, respectively. Following this reasoning, we expect that the critical ionic strength for the PDAC/PSS LbL system lies somewhere between 0 and 0.25 M NaCl.

These new results allow us to comment on the ongoing discussion regarding linear and exponential growth as it relates to rigid and soft films.^{20,21,24,28,34,62,63,65} It is most relevant to discuss

the data for the hydrated LbL films examined within their salt-adjusted solutions because it most accurately portrays the environment experienced by the LbL film during the assembly process. Here, the linearly growing PDAC/PSS LbL films assembled without added salt did not have a detectable T_g ; if the hydrated film had a T_g , then it would be outside of our current measurement range (likely above 110 °C). In contrast, the exponentially growing hydrated PDAC/PSS LbL films assembled with added salt did have a detectable T_g , albeit above room temperature. Because the T_g of the exponentially growing films is closer to room temperature than that of the linearly growing film, the mobility of polyelectrolytes within the exponentially growing film may be relatively higher. Enhanced mobility supports the “in and out” diffusion of polyelectrolytes observed for exponentially growing films.⁶⁶ In the present system studied, exponentially growing films were assembled in the presence of salt, which leads to fewer ion pairs than a linearly growing film assembled without added salt. Accordingly, the T_g of an exponentially growing film should be lower than that of a linearly growing film because the exponentially growing film, which has more loops and trains, has greater free volume.

CONCLUSION

The thermal properties of dry and hydrated PDAC/PSS LbL films assembled from solutions of varying ionic strength have been investigated using MDSC and

QCM-D. We demonstrate a distinct glass transition in exponentially growing films (assembled in the presence of salt), whereas no detectable glass transitions were observed in the linearly growing LbL films (assembled without added salt). The integration of MDSC with QCM-D results provides new insights into the structure and thermal properties of LbL films. Whereas thermal properties are sensitive to the terminal layer (PDAC or PSS) for thin films, bulk PDAC/PSS LbL films exhibited similar T_g values irrespective of their termination layer. QCM-D has been employed for the first time to probe thermal transitions for LbL films. The analysis of different QCM-D overtones yields an important tool in analyzing thermal transitions in LbL assemblies by studying subtle changes in film hydration and viscoelasticity as a function of penetration depth.

Our future work will focus on other LbL systems that grow linearly and exponentially, particularly those containing weak polyelectrolytes, which are sensitive to pH. We anticipate that techniques and analyses presented here can be applied to other thin films beyond LbL assemblies, such as neutral homopolymers. Temperature-controlled QCM-D is more sensitive to thermal transitions than MDSC and provides a potent tool for simultaneously examining minute changes in hydration and viscoelasticity. It is particularly useful for systems that contain a solvent such as water, whose presence may amplify changes in frequency and dissipation.

EXPERIMENTAL SECTION

Materials. Poly(diallyldimethylammonium chloride) (PDAC, $M_w = 350\,000\text{ g mol}^{-1}$) and poly(styrene sulfonate sodium salt) (PSS, $M_w = 500\,000\text{ g mol}^{-1}$) were purchased from Sigma Aldrich and Scientific Polymer Products, respectively. Poly(ethylene imine) (PEI, $M_w = 25\,000\text{ g mol}^{-1}$) was purchased from Polysciences, Inc. Teflon and quartz crystal substrates were purchased from McMaster Carr and Q-sense, respectively.

Preparation of Free-Standing Layer-by-Layer Assemblies. PDAC and PSS solutions were made from their respective homopolymers and 18.2 MΩ Milli-Q water at a concentration of 1 mg/mL. LbL assemblies were constructed using an automated slide stainer (HMS series, Carl Zeiss, Inc.). Teflon substrates used to fabricate free-standing LbL assemblies were cleaned using sonication for 15 min in ethanol, followed by 15 min sonication in deionized water. Teflon substrates were dipped in PDAC solution for 15 min, followed by three separate rinses with Milli-Q water for 2, 1, and 1 min, respectively. The substrates were then dipped in PSS solution for 15 min, followed by another series of water rinses as before. The ionic strength of assembly was varied from 0 to 1.25 M NaCl for all baths. The LbL films were then dried in ambient air and stored in a desiccator until further use. The films were isolated from their Teflon substrates (Figure 2) just before MDSC experiments.

Quartz Crystal Microbalance with Dissipation (QCM-D) Measurements. All QCM-D experiments were performed using the Q-sense E1 system. The gold-plated AT-cut quartz crystals were first plasma treated for 10 min followed by a 10 min immersion in a water/NH₄OH/H₂O₂ (5:1:1) mixture at 70 °C for 10 min, dried using

nitrogen, and then plasma treated as before. LbL film assembly was then carried out by first flowing 1 mg/mL PEI solution (pH 4.5) for 15 min. This initial layer was considered the zeroth layer and was used as a baseline for all QCM-D experiments. Then, 0.1 mg/mL PSS solution was passed over the crystal at a flow rate of 200 μL/min for 15 min, followed by a 5 min rinse using Milli-Q water. Then, 0.1 mg/mL PDAC solution was passed for 15 min, followed by rinsing as before. This procedure was repeated until the desired number of layers was achieved. LbL films made of PEI/(PSS/PDAC) assembled from 0.5 and 1.0 M NaCl were constructed in a similar fashion, and rinse solutions were of matching ionic strengths.

Quantification of QCM-D Data. The Sauerbrey equation, which relates change in frequency and the adsorbed mass, was used to provide initial guesses for future models:

$$M_{\text{qcm}} = -C \frac{\Delta F}{n} \quad (1)$$

where C is a sensitivity constant and n is the overtone number of the oscillating frequency ($n = 1, 3, 5, 7, 9, 11, 13$). The mass deposited on the QCM-D crystal is the coupled mass (*i.e.*, the mass of the adsorbed polymer including water). The validity of the Sauerbrey equation is limited to rigid films. For more viscoelastic films, more complex models have to be employed to capture changes in both frequency and dissipation. We have found the Sauerbrey equation to be a good first approximation for our LbL films. We have used the thickness and mass calculated from the Sauerbrey equation as an initial guess to model LbL film growth using the Voigt model.⁶⁷ We have found

that both models can be used with reasonable accuracy. Calculations were performed by taking all overtones ($n = 3-13$) into consideration using QSoft software (Q-sense). The decay of the evanescent wave (K) owing to dissipation in an aqueous medium is about 250 nm for the fundamental frequency (5 MHz for $n = 1$) according to the equation⁶⁷

$$K = \sqrt{\frac{\pi f \rho}{\eta}} \quad (2)$$

where ρ is the density and η is the viscosity of the fluid surrounding the crystal surface vibrating at a frequency f .

Modulated Differential Scanning Calorimetry (MDSC) Measurements. MDSC was performed on dry samples in a heat-cool-heat cycle. The sample weight ranged between 5 and 12 mg, depending on sample availability. Tzero aluminum pans and lids were used for dry LbL films and homopolymers, and Tzero hermetic pans and lids were used for hydrated samples. Dry homopolymers PDAC and PSS as well as dry PDAC/PSS LbL films were first held at 35 °C for 5 min in a nitrogen purge, then samples were ramped from 0 to 250 °C at a rate of 3 °C min⁻¹ with amplitude of 1 °C for a period of 60 s. Hydrated films were ramped from 0 to 115 °C at a rate of 2 °C min⁻¹ with amplitude of 1.272 °C for a period of 60 s. All MDSC thermograms are shown in "exotherm down" format.

Conflict of Interest: The authors declare no competing financial interest.

Acknowledgment. This material is based upon work supported by the National Science Foundation under Grant No. 1049706 and Texas A&M University start-up funds. We thank Dr. Nichole Zacharia for profilometer access. We thank Dr. Archana Jaiswal, Dr. Matthew Dixon, and Dr. Mark Poggi from Q-Sense for assistance with QCM-D data analysis.

Supporting Information Available: MDSC thermograms of hydrated PDAC and PSS homopolymers; MDSC thermogram of PDAC/PSS assembled from 1.0 M NaCl and hydrated in water with no added salt; table of fitting parameters for the QCM-D modeling. This material is available free of charge via the Internet at <http://pubs.acs.org>.

REFERENCES AND NOTES

- Laschewsky, A.; Mayer, B.; Wischerhoff, E.; Arys, X.; Bertrand, P.; Delcorte, A.; Jonas, A. A New Route to Thin Polymeric, Non-centrosymmetric Coatings. *Thin Solid Films* **1996**, *284*–285, 334–337.
- Langer, R. Drug Delivery and Targeting. *Nature* **1998**, *392*, 5–10.
- Peyratout, C. S.; Dähne, L. Tailor-Made Polyelectrolyte Microcapsules: From Multilayers to Smart Containers. *Angew. Chem., Int. Ed.* **2004**, *43*, 3762–3783.
- Constantine, C. A.; Mello, S. V.; Dupont, A.; Cao, X.; Santos, D.; Oliveira, O. N.; Strixino, F. T.; Pereira, E. C.; Cheng, T.-C.; Defrank, J. J.; *et al.* Layer-by-Layer Self-Assembled Chitosan/Poly(thiophene-3-acetic acid) and Organophosphorus Hydrolase Multilayers. *J. Am. Chem. Soc.* **2003**, *125*, 1805–1809.
- Decher, G.; Lehr, B.; Lowack, K.; Lvov, Y.; Schmitt, J. New Nanocomposite Films for Biosensors: Layer-by-Layer Adsorbed Films of Polyelectrolytes, Proteins or DNA. *Biosens. Bioelectron.* **1994**, *9*, 677–684.
- Cheung, J. H.; Fou, A. F.; Rubner, M. F. Molecular Self-Assembly of Conducting Polymers. *Thin Solid Films* **1994**, *244*, 985–989.
- Guzman, E.; Ritacco, H.; Rubio, J. E. F.; Rubio, R. G.; Ortega, F. Salt-Induced Changes in the Growth of Polyelectrolyte Layers of Poly(diallyl-dimethylammonium chloride) and Poly(4-styrene sulfonate of sodium). *Soft Matter* **2009**, *5*, 2130–2142.
- Liu, G.; Zou, S.; Fu, L.; Zhang, G. Roles of Chain Conformation and Interpenetration in the Growth of a Polyelectrolyte Multilayer. *J. Phys. Chem. B* **2008**, *112*, 4167–4171.
- Wong, J. E.; Zastrow, H.; Jaeger, W.; von Klitzing, R. Specific Ion versus Electrostatic Effects on the Construction of Polyelectrolyte Multilayers. *Langmuir* **2009**, *25*, 14061–14070.
- Schlenoff, J. B.; Dubas, S. T. Mechanism of Polyelectrolyte Multilayer Growth: Charge Overcompensation and Distribution. *Macromolecules* **2001**, *34*, 592–598.
- Steitz, R.; Leiner, V.; Siebrecht, R.; von Klitzing, R. Influence of the Ionic Strength on the Structure of Polyelectrolyte Films at the Solid/Liquid Interface. *Colloids Surf. A* **2000**, *163*, 63–70.
- Lee, D.; Nolte, A. J.; Kunz, A. L.; Rubner, M. F.; Cohen, R. E. pH-Induced Hysteretic Gating of Track-Etched Polycarbonate Membranes: Swelling/Deswelling Behavior of Polyelectrolyte Multilayers in Confined Geometry. *J. Am. Chem. Soc.* **2006**, *128*, 8521–8529.
- Shiratori, S. S.; Rubner, M. F. pH-Dependent Thickness Behavior of Sequentially Adsorbed Layers of Weak Polyelectrolytes. *Macromolecules* **2000**, *33*, 4213–4219.
- Lvov, Y.; Antipov, A. A.; Mamedov, A.; Möhwald, H.; Sukhorukov, G. B. Urea Encapsulation in Nanoorganized Microshells. *Nano Lett.* **2001**, *1*, 125–128.
- Büscher, K.; Graf, K.; Ahrens, H.; Helm, C. A. Influence of Adsorption Conditions on the Structure of Polyelectrolyte Multilayers. *Langmuir* **2002**, *18*, 3585–3591.
- Tan, H. L.; McMurdo, M. J.; Pan, G.; Van Patten, P. G. Temperature Dependence of Polyelectrolyte Multilayer Assembly. *Langmuir* **2003**, *19*, 9311–9314.
- Gopinadhan, M.; Ahrens, H.; Günther, J.-U.; Steitz, R.; Helm, C. A. Approaching the Precipitation Temperature of the Deposition Solution and the Effects on the Internal Order of Polyelectrolyte Multilayers. *Macromolecules* **2005**, *38*, 5228–5235.
- Secrist, K. E.; Nolte, A. J. Humidity Swelling/Deswelling Hysteresis in a Polyelectrolyte Multilayer Film. *Macromolecules* **2011**, *44*, 2859–2865.
- Lavalle, P.; Picart, C.; Mutterer, J.; Gergely, C.; Reiss, H.; Voegel, J. C.; Senger, B.; Schaaf, P. Modeling the Buildup of Polyelectrolyte Multilayer Films Having Exponential Growth. *J. Phys. Chem. B* **2004**, *108*, 635–648.
- Mermut, O.; Lefebvre, J.; Gray, D. G.; Barrett, C. J. Structural and Mechanical Properties of Polyelectrolyte Multilayer Films Studied by AFM. *Macromolecules* **2003**, *36*, 8819–8824.
- Francius, G.; Hemmerlé, J.; Ball, V.; Lavalle, P.; Picart, C.; Voegel, J.-C.; Schaaf, P.; Senger, B. Stiffening of Soft Polyelectrolyte Architectures by Multilayer Capping Evidenced by Viscoelastic Analysis of AFM Indentation Measurements. *J. Phys. Chem. C* **2007**, *111*, 8299–8306.
- Richert, L.; Engler, A. J.; Discher, D. E.; Picart, C. Elasticity of Native and Cross-Linked Polyelectrolyte Multilayer Films. *Biomacromolecules* **2004**, *5*, 1908–1916.
- von Klitzing, R. Internal Structure of Polyelectrolyte Multilayer Assemblies. *Phys. Chem. Chem. Phys.* **2006**, *8*, 5012–5033.
- Gao, C.; Leporatti, S.; Moya, S.; Donath, E.; Möhwald, H. Stability and Mechanical Properties of Polyelectrolyte Capsules Obtained by Stepwise Assembly of Poly(styrenesulfonate sodium salt) and Poly(diallyldimethyl ammonium) Chloride onto Melamine Resin Particles. *Langmuir* **2001**, *17*, 3491–3495.
- Jaber, J. A.; Schlenoff, J. B. Mechanical Properties of Reversibly Cross-Linked Ultrathin Polyelectrolyte Complexes. *J. Am. Chem. Soc.* **2006**, *128*, 2940–2947.
- Jaber, J. A.; Schlenoff, J. B. Dynamic Viscoelasticity in Polyelectrolyte Multilayers: Nanodamping. *Chem. Mater.* **2006**, *18*, 5768–5773.
- Nolte, A. J.; Cohen, R. E.; Rubner, M. F. A Two-Plate Buckling Technique for Thin Film Modulus Measurements: Applications to Polyelectrolyte Multilayers. *Macromolecules* **2006**, *39*, 4841–4847.
- Nolte, A. J.; Rubner, M. F.; Cohen, R. E. Determining the Young's Modulus of Polyelectrolyte Multilayer Films via Stress-Induced Mechanical Buckling Instabilities. *Macromolecules* **2005**, *38*, 5367–5370.
- Pavoor, P. V.; Bellare, A.; Strom, A.; Yang, D.; Cohen, R. E. Mechanical Characterization of Polyelectrolyte Multilayers

- Using Quasi-Static Nanoindentation. *Macromolecules* **2004**, *37*, 4865–4871.
30. Salomäki, M.; Laiho, T.; Kankare, J. Counteranion-Controlled Properties of Polyelectrolyte Multilayers. *Macromolecules* **2004**, *37*, 9585–9590.
 31. Salomäki, M.; Loikas, K.; Kankare, J. Effect of Polyelectrolyte Multilayers on the Response of a Quartz Crystal Microbalance. *Anal. Chem.* **2003**, *75*, 5895–5904.
 32. Schönhoff, M.; Ball, V.; Bausch, A. R.; Dejugnat, C.; Delorme, N.; Glinel, K.; von Klitzing, R.; Steitz, R. Hydration and Internal Properties of Polyelectrolyte Multilayers. *Colloids Surf. A* **2007**, *303*, 14–29.
 33. Mueller, R.; Köhler, K.; Weinkamer, R.; Sukhorukov, G.; Fery, A. Melting of PDADMAC/PSS Capsules Investigated with AFM Force Spectroscopy. *Macromolecules* **2005**, *38*, 9766–9771.
 34. Köhler, K.; Möhwald, H.; Sukhorukov, G. B. Thermal Behavior of Polyelectrolyte Multilayer Microcapsules: 2. Insight into Molecular Mechanisms for the PDADMAC/PSS System. *J. Phys. Chem. B* **2006**, *110*, 24002–24010.
 35. Nazaran, P.; Bosio, V.; Jaeger, W.; Anghel, D. F.; von Klitzing, R. Lateral Mobility of Polyelectrolyte Chains in Multilayers. *J. Phys. Chem. B* **2007**, *111*, 8572–8581.
 36. Ghostine, R. A.; Schlenoff, J. B. Ion Diffusion Coefficients through Polyelectrolyte Multilayers: Temperature and Charge Dependence. *Langmuir* **2011**, *27*, 8241–8247.
 37. Salomäki, M.; Vinokurov, I. A.; Kankare, J. Effect of Temperature on the Buildup of Polyelectrolyte Multilayers. *Langmuir* **2005**, *21*, 11232–11240.
 38. Jang, W.-S.; Jensen, A. T.; Lutkenhaus, J. L. Confinement Effects on Cross-Linking within Electrostatic Layer-by-Layer Assemblies Containing Poly(allylamine hydrochloride) and Poly(acrylic acid). *Macromolecules* **2010**, *43*, 9473–9479.
 39. Shao, L.; Lutkenhaus, J. L. Thermochemical Properties of Free-Standing Electrostatic Layer-by-Layer Assemblies Containing Poly(allylamine hydrochloride) and Poly(acrylic acid). *Soft Matter* **2010**, *6*, 3363–3369.
 40. Lutkenhaus, J. L.; McEnnis, K.; Hammond, P. T. Tuning the Glass Transition of and Ion Transport within Hydrogen-Bonded Layer-by-Layer Assemblies. *Macromolecules* **2007**, *40*, 8367–8373.
 41. Lutkenhaus, J. L.; Hrabak, K. D.; McEnnis, K.; Hammond, P. T. Elastomeric Flexible Free-Standing Hydrogen-Bonded Nanoscale Assemblies. *J. Am. Chem. Soc.* **2005**, *127*, 17228–17234.
 42. Gu, X. K.; Knorr, D. B.; Wang, G. J.; Overney, R. M. Local Thermal-Mechanical Analysis of Ultrathin Interfacially Mixed Poly(ethylene oxide)/Poly(acrylic acid) Layer-by-Layer Electrolyte Assemblies. *Thin Solid Films* **2011**, *519*, 5955–5961.
 43. Iturri Ramos, J. J.; Stahl, S.; Richter, R. P.; Moya, S. E. Water Content and Buildup of Poly(diallyldimethylammonium chloride)/Poly(sodium 4-styrenesulfonate) and Poly(allylamine hydrochloride)/Poly(sodium 4-styrenesulfonate) Polyelectrolyte Multilayers Studied by an *In Situ* Combination of a Quartz Crystal Microbalance with Dissipation Monitoring and Spectroscopic Ellipsometry. *Macromolecules* **2010**, *43*, 9063–9070.
 44. Liu, G.; Hou, Y.; Xiao, X.; Zhang, G. Specific Anion Effects on the Growth of a Polyelectrolyte Multilayer in Single and Mixed Electrolyte Solutions Investigated with Quartz Crystal Microbalance. *J. Phys. Chem. B* **2010**, *114*, 9987–9993.
 45. Picart, C.; Mutterer, J.; Richert, L.; Luo, Y.; Prestwich, G. D.; Schaaf, P.; Voegel, J.-C.; Lavalley, P. Molecular Basis for the Explanation of the Exponential Growth of Polyelectrolyte Multilayers. *Proc. Natl. Acad. Sci. U.S.A.* **2002**, *99*, 12531–12535.
 46. Ishida, N.; Biggs, S. Direct Observation of the Phase Transition for a Poly(*N*-isopropylacrylamide) Layer Grafted onto a Solid Surface by AFM and QCM-D. *Langmuir* **2007**, *23*, 11083–11088.
 47. Martin, S. J.; Granstaff, V. E.; Frye, G. C. Characterization of a Quartz Crystal Microbalance with Simultaneous Mass and Liquid Loading. *Anal. Chem.* **1991**, *63*, 2272–2281.
 48. Zhu, D. M.; Fang, J. J.; Wu, B.; Du, X. B. Viscoelastic Response and Profile of Adsorbed Molecules Probed by Quartz Crystal Microbalance. *Phys. Rev. E* **2008**, *77*.
 49. Choi, I.; Suntivich, R.; Plamper, F. A.; Synatschke, C. V.; Müller, A. H. E.; Tsukruk, V. V. pH-Controlled Exponential and Linear Growing Modes of Layer-by-Layer Assemblies of Star Polyelectrolytes. *J. Am. Chem. Soc.* **2011**, *133*, 9592–9606.
 50. Köhler, K.; Biesheuvel, P. M.; Weinkamer, R.; Möhwald, H.; Sukhorukov, G. B. Salt-Induced Swelling-to-Shrinking Transition in Polyelectrolyte Multilayer Capsules. *Phys. Rev. Lett.* **2006**, *97*.
 51. Köhler, K.; Shchukin, D. G.; Möhwald, H.; Sukhorukov, G. B. Thermal Behavior of Polyelectrolyte Multilayer Microcapsules. 1. The Effect of Odd and Even Layer Number. *J. Phys. Chem. B* **2005**, *109*, 18250–18259.
 52. Forrest, J. A.; Svanberg, C.; Révész, K.; Rodahl, M.; Torell, L. M.; Kasemo, B. Relaxation Dynamics in Ultrathin Polymer Films. *Phys. Rev. E* **1998**, *58*, R1226.
 53. Forrest, J. A.; Svanberg, C.; Révész, K.; Rodahl, M.; Torell, L. M.; Kasemo, B. Relaxation Dynamics in Ultrathin Polymer Films. *Phys. Rev. E* **1998**, *58*, R1226.
 54. Soltwedel, O.; Ivanova, O.; Nestler, P.; Müller, M.; Köhler, R.; Helm, C. A. Interdiffusion in Polyelectrolyte Multilayers. *Macromolecules* **2010**, *43*, 7288–7293.
 55. Yeo, S. C.; Eisenberg, A. Effect of Ion Placement and Structure on Properties of Plasticized Polyelectrolytes. *J. Macromol. Sci., Part B: Phys.* **1977**, *13*, 441–484.
 56. Weber, N.; Unterlass, M. M.; Tauer, K. High Ionic Strength Promotes the Formation of Spherical Copolymer Particles. *Macromol. Chem. Phys.* **2011**, *212*, 2071–2086.
 57. M'Bareck, C. O.; Nguyen, Q. T.; Metayer, M.; Saiter, J. M.; Garda, M. R. Poly(acrylic acid) and Poly(sodium styrene-sulfonate) Compatibility by Fourier Transform Infrared and Differential Scanning Calorimetry. *Polymer* **2004**, *45*, 4181–4187.
 58. Imre, Á. W.; Schönhoff, M.; Cramer, C. A. Conductivity Study and Calorimetric Analysis of Dried Poly(sodium 4-styrene sulfonate)/Poly(diallyldimethylammonium chloride) Polyelectrolyte Complexes. *J. Chem. Phys.* **2008**, *128*, 134905.
 59. Farhat, T.; Yassin, G.; Dubas, S. T.; Schlenoff, J. B. Water and Ion Pairing in Polyelectrolyte Multilayers. *Langmuir* **1999**, *15*, 6621–6623.
 60. Chollakup, R.; Smitthipong, W.; Eisenbach, C. D.; Tirrell, M. Phase Behavior and Coacervation of Aqueous Poly(acrylic acid)-Poly(allylamine) Solutions. *Macromolecules* **2010**, *43*, 2518–2528.
 61. Schlenoff, J. B.; Ly, H.; Li, M. Charge and Mass Balance in Polyelectrolyte Multilayers. *J. Am. Chem. Soc.* **1998**, *120*, 7626–7634.
 62. Cerda, J. J.; Qiao, B.; Holm, C. Understanding Polyelectrolyte Multilayers: An Open Challenge for Simulations. *Soft Matter* **2009**, *5*, 4412–4425.
 63. Kovacevic, D.; van der Burgh, S.; de Keizer, A.; Cohen Stuart, M. A. Kinetics of Formation and Dissolution of Weak Polyelectrolyte Multilayers: Role of Salt and Free Polyions. *Langmuir* **2002**, *18*, 5607–5612.
 64. Kovacevic, D.; van der Burgh, S.; de Keizer, A.; Cohen Stuart, M. A. Specific Ionic Effects on Weak Polyelectrolyte Multilayer Formation. *J. Phys. Chem. B* **2003**, *107*, 7998–8002.
 65. Voinova, M. V.; Rodahl, M.; Jonson, M.; Kasemo, B. Viscoelastic Acoustic Response of Layered Polymer Films at Fluid-Solid Interfaces: Continuum Mechanics Approach. *Phys. Scr.* **1999**, *59*, 391.
 66. Kanazawa, K. K.; Gordon, J. G. Frequency of a Quartz Microbalance in Contact with Liquid. *Anal. Chem.* **1985**, *57*, 1770–1771.
 67. Kanazawa, K. K.; Gordon, J. G. The Oscillation Frequency of a Quartz Resonator in Contact with Liquid. *Anal. Chim. Acta* **1985**, *175*, 99–105.